Def Sci J, Vol 39, No. 4, October 1989, pp 335-352

# Growth of High-Quality *GaAs* by MBE

Naresh Chand

*AT&T Bell Laboratories, 600 Mountain Avenue*
*Murray Hill, New Jersey 07974, USA*

**ABSTRACT**

This paper reviews the requirements and current practices in the molecular beam epitaxial (MBE) growth of high-quality *GaAs*. High-quality growth of *GaAs* means excellent control on the growth process and the excellent surface, structural, electrical and optical properties of the deposited *GaAs*. Background material is presented about the MBE technique, the MBE system and its initial preparation for growth, molecular-beam source materials, substrate preparation and the growth conditions. The importance of meticulousness at every step is emphasized. Then, to illustrate that the MBE-*GaAs* has reached a level of perfection, experimental data is presented which shows an excellent control on the growth rate and its lateral uniformity ($\pm$ 0.75 per cent), the presence of very low-level of background impurities ($\sim$ low $10^{13}$ $cm^{-3}$) and high electron mobilities ($\mu_{peak} \sim 3 \times 10^5$ $cm^2$ $V^{-1}s^{-1}$ at 42 K for $n \sim 3 \times 10^{13}$ $cm^{-3}$). In addition, we show that MBE-*GaAs* is intrinsically free from electron and hole deep traps. Chemical impurities in the impure arsenic source are shown to be the main limiting factors in determining the transport and optical properties and formation of deep centers in MBE-*GaAs*. Such chemical impurities may, however, originate from other sources as well.

## 1. INTRODUCTION

Following A.Y. Cho's pioneering work in the development of molecular beam epitaxy (MBE) as a thin layer growth technique in the early 1970's, MBE has now become a viable production technique despite the initial high capital investment. MBE dominates in the preparation of semiconductors with tailored electrical properties that do not exist in nature for the basic and applied research work. MBE is solely responsible for the realisation and development of superlattices, quantum wells and a great many new devices and concepts[1].

Received 21 July 1989

The MBE technique is one of the fastest developing areas of research encompassing many disciplines and bringing together experts from many fields. Today, in the western world and in Japan, there is no major industry or university without an MBE program.

Compared to other epitaxial growth methods, MBE is distinguished by its low growth rate (typically 1-3 Å/s for *GaAs*), low growth temperature ($\lesssim 630$°C for *GaAs*), the ability of abrupt initiation or cessation of growth, smoothing of the surface of the growing crystal during growth down to atomic steps, and the capability for *in situ* analysis. As a result, the MBE technique provides reproducible control over composition, thickness, and doping profile in the direction of growth on an atomic scale, with very high lateral uniformity. Although the major MBE effort has been, and still is, on the III-V compounds, primarily *AlGaAs/GaAs*, the technique is finding its widespread applications for other material systems such as *Si, Ge,* and semiconductors in combination with insulators and/or metals, and more recently superconductors. The goal of the present article is to focus on the *AlGaAs/GaAs* material system and review the current practices for the growth of high-quality *GaAs* and *AlGaAs* by MBE.

## 2. MBE TECHNIQUE

There are a number of excellent review articles and books[1-7] which discuss various aspects of MBE, including its applications, in great detail. Briefly, MBE is an epitaxial growth process involving the reaction of one or more thermal beams of atoms or molecules with a crystalline surface under ultrahigh vacuum conditions. As shown schematically in Fig. 1 for *AlGaAs/GaAs*, the molecular beams are generated from sources of the Knudsen-

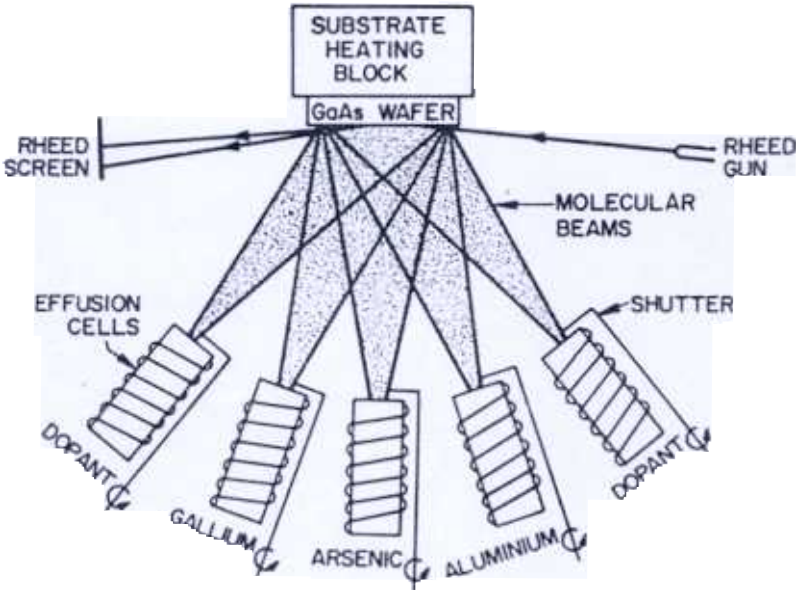


**Figure 1. A schematic illustration of the MBE growth chamber.**

effusion-cell type, whose temperatures are accurately controlled to $\pm$ 0.5°C. Each source is provided with an externally controlled individual shutter. Operation of these shutters permits rapid changing of the beam species in order to abruptly alter the composition and/or doping of the growing film. For a 1 μm/hr growth rate, the shutter operation is faster than the time needed for the growth of a monolayer. Thus, atomically abrupt interfaces between two different materials can be realised, if diffusion and surface accumulation are negligible. *Si* and *Be* are the normally used *n*-and *p*-type dopants in *GaAs* respectively.

Freshly etched substrates with a thin protective oxide are loaded into the MBE system through an air-lock where the substrate is first outgassed at 300–400°C for ~ 30 min. The cells are properly outgassed before commencing the growth. At the same time, the substrate is heated in the growth chamber to desorb the surface oxide, which for *GaAs* occurs between 580–600°C, and is monitored by *in situ* reflection high-energy electron diffraction (RHEED) shown in Fig. 1. At this point, the substrate is ready for growth which is started by opening the necessary cell shutters. The growth is also monitored by *in situ* RHEED. The growth is carried out under excess arsenic flux and the growth rate is determined by the arrival rate of *Ga* and *Al* atoms.

The crystal growth by MBE is influenced by surface kinetics and some impurities have very low sticking coefficients. But unlike some other growth techniques, such as liquid phase epitaxy (LPE), MBE does not provide any inherent mechanism of rejecting those unwanted impurities which have high sticking coefficients from being incorporated into the grown layers, and the surface of the substrate cannot be etched-back just before the growth. In addition, since the growth takes place under excess group V atomic or molecular flux, defects such as group III vacancies can be easily introduced in the layer grown under less than optimum conditions. Despite these different growth mechanisms, the quality of MBE epitaxial layers, especially in the *GaAs* technology, has now become the state-of-the-art standard. MBE-grown *GaAs* layers are purer than those grown by other techniques as determined by the presence of residual impurities, deep level defects and the electron mobilities. Residual acceptor density in MBE-*GaAs* as low as $2 \times 10^{13}$ cm$^{-3}$, and electron mobilities $> 2 \times 10^5$ cm$^2$ V$^{-1}$s$^{-1}$ at 77 K and $\sim 3 \times 10^5$ cm$^2$ V$^{-1}$s$^{-1}$ at 42 K for an electron density of $3 \times 10^{13}$ cm$^{-3}$ have been obtained[8]. Similar high electron mobilities have also been obtained in unintentionally doped *GaAs*, grown by gas source MBE[9]. Most recently, in modulation-doped heterostructures, two-dimensional electron gas (2-DEG) mobility as high as $10^7$ cm$^2$ V$^{-1}$s$^{-1}$ at $< 2$ K was obtained by Pfeiffer and coworkers[10] at Bell Laboratories. These high mobility results can not be obtained unless great care is taken at every step from fabrication of the MBE system to the final stage of the MBE growth. A brief discussion of the various steps is presented in the following sections.

## 3. THE MBE SYSTEM

The MBE system must be ultra clean, leak-proof and capable of holding ultra high vacuum with a base pressure of $10^{-11}$ torr. There are four main manufacturers of the MBE system: Varian in the USA, ISA Riber in France, VG Semicon in England and Alneva in Japan. Growth of high purity *GaAs* has been demonstrated in the MBE systems manufactured by first three of them[8-14]. The results, however, vary from system to system, and depend largely on the history of the MBE system and dedication of the crystal grower. A source of impurities once introduced inside the MBE system is difficult to be detected and removed. Any part which is going to be hot in the MBE system must be ultra clean. To ensure perfection, it is advisable for the crystal grower to reclean the hardware before it is installed. The vacuum parts are handled with clean powder free gloves, clean tools and with a face mask on.

For production purposes, it is advisable to install the MBE system in a class 100 or better clean room to reduce surface defect density. For research purposes, this is not essential. Growth of record high purity *GaAs* has been carried out in several laboratories[8,10] where the machine is installed in ordinary laboratory space. As shown in Fig. 2, the MBE machine is installed in an ordinary room but the substrate introduction chamber is

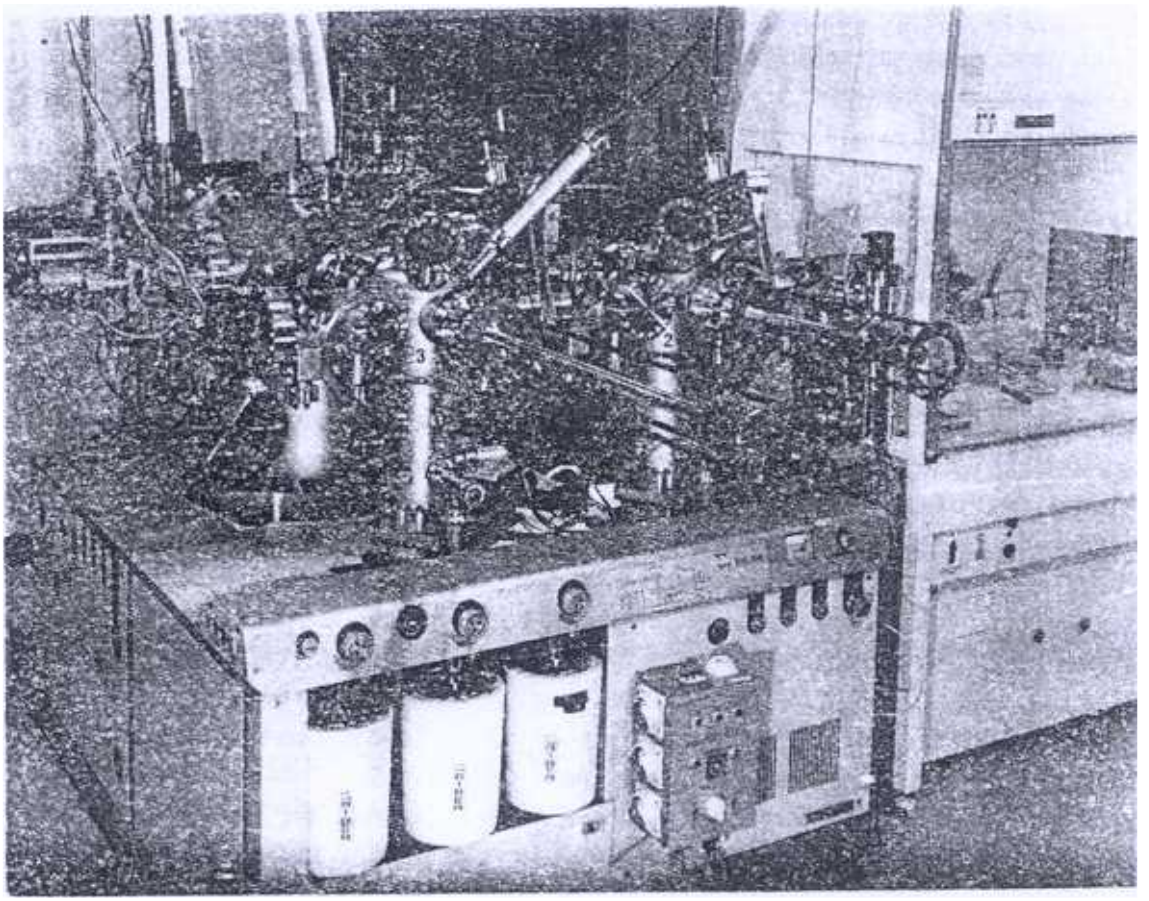

**2. A III-V Riber 3200P MBE system, based on modular design, illustrating the configuration of the major components.**

connected to a class 10 laminar flow station where the loading or unloading of the wafers is done. This laminar flow station itself is connected by a pass-through window to another class 10 laminar flow station where the chemical cleaning of the substrate is done. In this way, the substrates always remain in a clean environment from the cleaning stage to the removal of the wafers from the MBE system after the growth.

The MBE system shown in Fig. 2 is based on a modular design. This design allows the user to flexibly configure the system for a specific requirement. Multiple chambers for deposition, substrate introduction, preparation, and analysis purposes can be interconnected easily while maintaining complete isolation between them through gate valves. The *Mo* substrate holders with substrates are loaded on a cassette which moves through a railing system on the modutrack. The substrate holder is picked up from the cassette by a magnetically coupled transfer rod and transferred to the desired position in the growth chamber or elsewhere. The system in Fig. 2 has four chambers numbered 1, 2, 3 and 4. The cell temperatures and the cell shutter positions are controlled by an AT&T 6300 computer.

After the installation of an MBE system, the initial preparation of the growth chamber involves a careful series of long bakes and thorough outgassing of the furnaces, crucibles, substrate heater filaments, molybdenum substrate holders, and ion-gauge filaments. Baking or outgassing does not commence until the system is thoroughly leak-proof. A quadrupole mass spectrometer in the growth chamber is very useful for leak detection and analysing the residual gases. The exact baking or outgassing procedure varies from laboratory to laboratory. Numerous approaches used can be found in the literature[12-15]. The

baking and outgassing procedure outlined by ISA Riber in their system manual was found to be more than adequate. In fact, the system was never baked for more than five days at any time to prolong the system life. After each time the system is opened, it must be rebaked. The goal is to pump out the residual gases, comprising mainly $H_2O$, $N_2$, $CO$, $CO_2$ and $H_2$, so that a base pressure of $10^{-11}$ torr is obtained when the chamber is at room temperature. After the system bake out, the titanium sublimation pump (TSP), the ion pump and the lower half of the growth chamber are allowed to cool first so that the cooling drives the residual gases toward the ion pump, away from the sources and substrate heater assembly. Efforts are made to open the growth chamber as infrequently as possible. The system is filled with dry $N_2$ gas before opening. All necessary preparations are done to minimise the system opening time and subsequent baking period. The longer the system remains open, the more water and other gases are absorbed inside the system, requiring longer baking.

MBE growth of high-quality thin layers requires a good thermal isolation between the individual effusion cells and the rest of the vacuum chamber to minimise outgassing from the walls, and the transfer of heat from cell to cell. This is achieved by cooling the panel which surrounds the effusion cells with liquid nitrogen (LN). Besides the cells panel, the epitaxy chamber and TSP are also cooled with LN. Cooling with LN also provides cryogenic pumping and increases the effectiveness of TSP leading to a tremendous increase in the pumping speed of the system. For the growth of high-quality *GaAs*, the current practice in many laboratories, including AT&T Bell Laboratory, is to constantly cool the system with LN and keep the cells heated at suitable standby temperatures. This reduces the downtime of the system and keeps the source materials clean. A great risk, however, is taken in this mode of operation. An accidental leak in the system, while the system is unattended and trapped with LN with hot cells, will severely damage the system. Atomospheric gases will react with hot filaments and source materials. As a result, all the cells and substrate filament will have to be replaced, and the system will require a thorough cleaning with extended bake out. Also, a power failure when the *Ga* and *Al* cells are hot and the system is trapped with LN, may damage these cells. Aluminum wets the pyrolitic boron nitride (PBN) crucible and it contracts on cooling, whereas *Ga* expands on cooling. Thus, if the crucibles are overfilled with *Ga* and *Al*, fast cooling by LN after the power failure will crack the PBN crucibles. The *Ga* or *Al* charge will leak through the broken crucible and react with the tantalum heater assembly of the cell. To prevent this, use of double wall PBN crucibles is preferred and a back-up power supply for *Ga* and *Al* cells are used. Too much *Al* in the crucible, in any case, is highly undesirable.

## 4. EVAPORATION SOURCES

The purity of the MBE-grown layers, in general, cannot be better than the quality of the evaporation sources used, as the growth mechanism does not discriminate between desired and undesired species. Therefore, the purest available source materials are a prerequisite. Before loading the source materials, the PBN crucible and the heater assembly of the cells are thoroughly outgassed, as discussed earlier, otherwise the sources will be contaminated. Presently, 8N purity *Ga*, 7N purity *Al* and 7N purity *As* are commercially available, and these purities are considered adequate to grow the state-of-the-art (*Al*) *GaAs*. Arsenic slugs are now available which just fit the PBN crucibles. These slugs are more desirable than the chunks. By replacing 6N grade double refined *As* chunks with a 7N grade *As* slug, residual acceptor density in our system was reduced by over two orders of magnitude. Gallium and aluminum are also available in large size slugs which are preferred for reason of reduced reactive surface area.

Some crystal growers load all source materials without any chemical treatment. We prefer to degrease and chemically etch the *Ga* and *Al* slugs just before loading. Gallium is etched in *HCl* and *Al* separately in *KOH* and *HF* solutions. In the present case for *Si*, a large piece of *Si* with $\rho = 5000$ Ω-cm was hammered into pieces and a small uncontaminated piece from the middle of the crystal was used for the *n*-type doping. After loading the charges, the initial pumping speed is kept slow, especially if *Ga* is freshly loaded and is in liquid form. During this period the shutters should remain open. After leak checking and baking the system, the cells are individually outgassed. Following the technique of Cho[16], preference was given to outgas the cells first at low temperatures (100°C for *As* and 600°C for other cells) with dry $N_2$ flowing through the shrouds. When the shrouds become hot, which is also shown by hot $N_2$ coming out, the outgassing is stopped and the system is allowed to cool to the room temperature. The system is then trapped with LN and the cells are reheated to be outgassed at about 100°C above the maximum operating temperature (except *As*) with and without shutters closed.

For high-quality growth of *GaAs*, the cells are left idling at 700–900°C (*As* cell at 100–150°C) and the LN cools the system continuously. The *As* cells are operated at much lower temperatures (200–300°C) as compared to other cells. Over a period of time, they may gather unwanted deposits from other cells or elsewhere. After the *As* cells are empty, outgassing was done at ~ 1400°C for several hours to make them ready for fresh recharging. This outgassing of *As* cells cannot be done after the arsenic is loaded. Before reinstalling the recharged cells in the MBE system, the cells housing in the cryoshroud and the shutters are thoroughly vacuum-cleaned. Sometimes the deposited material is so stiff that it has to be scratched with a stainless steel or glass tube and sucked by a vacuum cleaner connected on the other side of the tube.

## 5. SUBSTRATE PREPARATION

Historically, in Cho's words[16], 'substrate preparation is the single most important step for successful MBE growth'. He spends countless hours emphasizing the importance of this step to new crystal growers. In the development of MBE, he personally polished and cleaned over 2000 wafers in order to study the effect of substrate preparation on crystal growth quality[16]. This was also the last step he delegated to his supporting staff.

The precise details of the substrate preparation vary from user to user. The present quality of the commercially available wafers is far superior than it was a decade ago, and therefore, the substrate preparation is relatively easier now. The goal is to produce a surface free from metallic and organic impurities and protected from atmospheric contamination by a thin passivating oxide layer. Besides the high purity chemical solutions, an adequate supply of high resistivity (18 M Ω-cm) running deionised (DI) water is essential. The beakers and tweezers are kept very clean. The beakers used for etching should remain filled with DI water and tweezers should remain in water while not in use. Plastic tweezers are preferable to metallic ones.

After blowing away any dust particle from the surface, the *GaAs* substrate is degreased sequentially in trichloroethylene, acetone and methanol, followed by a rinse in running DI water. It is advisable to use a teflon or quartz substrate holder to avoid repeated contact of tweezers with the substrate. The substrate is then etched in a basic ($5NH_4OH$: $2H_2O_2$: $10H_2O$ for 2 min) or in an acidic (4 $H_2SO_4$: $1H_2O_2$: $1H_2O$ for 5 min) or in both solutions, followed by a rinse in DI water. The oxide layer deposited during chemical etching is then removed by etching in *HCl*. Finally, the wafer is rinsed in water for 1 to 2 min which also

deposits a thin protective oxide layer, and then dried by spinning or by dry $N_2$. The cleaned substrates are then mounted on the molybdenum blocks using indium. The surface tension of the molten *In* is sufficient to hold the sample on the heating block. If the growth is to be carried out on full size standard substrates, *In*-free *Mo* blocks can be used. All operations in air are carried out under dust-free conditions. Immediately after substrate mounting, the loaded *Mo* blocks are placed in the vacuum system to avoid particulate contamination.

## 6. GROWTH CONDITIONS

The growth conditions for obtaining high-quality *GaAs* epitaxial layers with mirror-shiny surfaces are well-established with growth rates up to 10 μm/hr at a substrate temperature of 620°C. Such growth will take place if the *As/Ga* flux ratio is above a certain value, which is a function of substrate temperature and surface orientation, giving an '*As*-stabilised' surface structure[1-3]. The typical growth rate used is 1 μm/hr. RHEED is used for examining the quality of growth while it is taking place. RHEED provides considerable information[1-5] about surface topography, with characteristic diffraction features indicating the presence of microscopic roughness, twinning, or oriented inclined facets on an otherwise flat surface. By studying the RHEED oscillations, discussed in detail elsewhere[5], the growth conditions can further be optimized, and the absolute growth rate and the *AlAs* mole-fraction in *AlGaAs* can easily be determined. The occasionally obtained rough surface of the grown *GaAs* layer is an indication of incomplete oxide desorption, or overheating of the substrate during growth, or insufficient arsenic flux. *GaAs* layers grown at 600–620°C with just sufficient *As/Ga* flux ratio in '*As*-stabilised' condition, have better purity and luminescence properties. The quality of *AlGaAs* is better when it is grown at 700°C.

Substrate temperature measurements can vary widely from system to system depending on a variety of factors, such as type and placing of thermocouples, *Mo* block, substrate type, and emissivity values assumed when using pyrometric methods. The substrate temperature may vary as the growth proceeds due to change in surface emissivity of the *Mo* block and heat absorption by the substrate. Here too, *in situ* RHEED is very helpful in providing rough calibration of the thermocouple, emissivity and in determining the right growth temperature. Fortunately, for high-quality growth of *GaAs*, there is a wide window of growth conditions and experience helps in determining the optimum values for a given MBE system.

## 7. CONTROL ON GROWTH RATE AND LATERAL UNIFORMITY

The growth rate in an MBE system remains fairly constant for given cell temperatures provided that, (a) the thermocouples are in intimate contact with the bottom of the PBN crucibles which contain the evaporation source materials, (b) the cell temperatures are controlled within $\pm < 0.5$°C, (c) the cells have sufficient charge, and (d) adequate and steady LN flows through the cryoshrouds. The growth rate is calibrated more accurately by *in situ* flux measurements which are carried out just before and after the growth run using an ion-gauge at the position of the growth. Modern MBE systems are equipped with a manipulator which can bring either the substrate or the ion-gauge to the growth position. Minor adjustments in the cell temperatures can be made to obtain the right fluxes for a given growth rate. The ion-gauge measures the beam equivalent pressure (BEP) and, if necessary, the absolute fluxes can be deduced from the grown film thickness. The fluxes are an exponential function of cell temperatures, and *GaAs* growth rate is directly

proportional to the *Ga* flux. Therefore, with a single thickness calibration of *GaAs*, the growth rate of *GaAs* can be varied easily by varying the *Ga* flux in a highly controlled manner. For $Al_xGa_{1-x}As$, the *AlAs* mole fraction, $x$, can be determined by the relation

$$x = \frac{G(Al_xGa_{1-x}As) - G(GaAs)}{G(Al_xGa_{1-x}As)} \tag{1}$$

where $G(Al_xGa_{1-x}As)$ and $G(GaAs)$ are the growth rates of $Al_xGa_{1-x}As$ and *GaAs* respectively. The value of $x$ can also be determined by photoluminescence or x-ray diffraction.

In our particular Riber 3200 system, the distance between the cells and the substrate is 30 mm more than their standard distance of 120 mm. This separation was kept larger to obtain better lateral uniformity of growth. As shown schematically in Fig. 3(a), the system

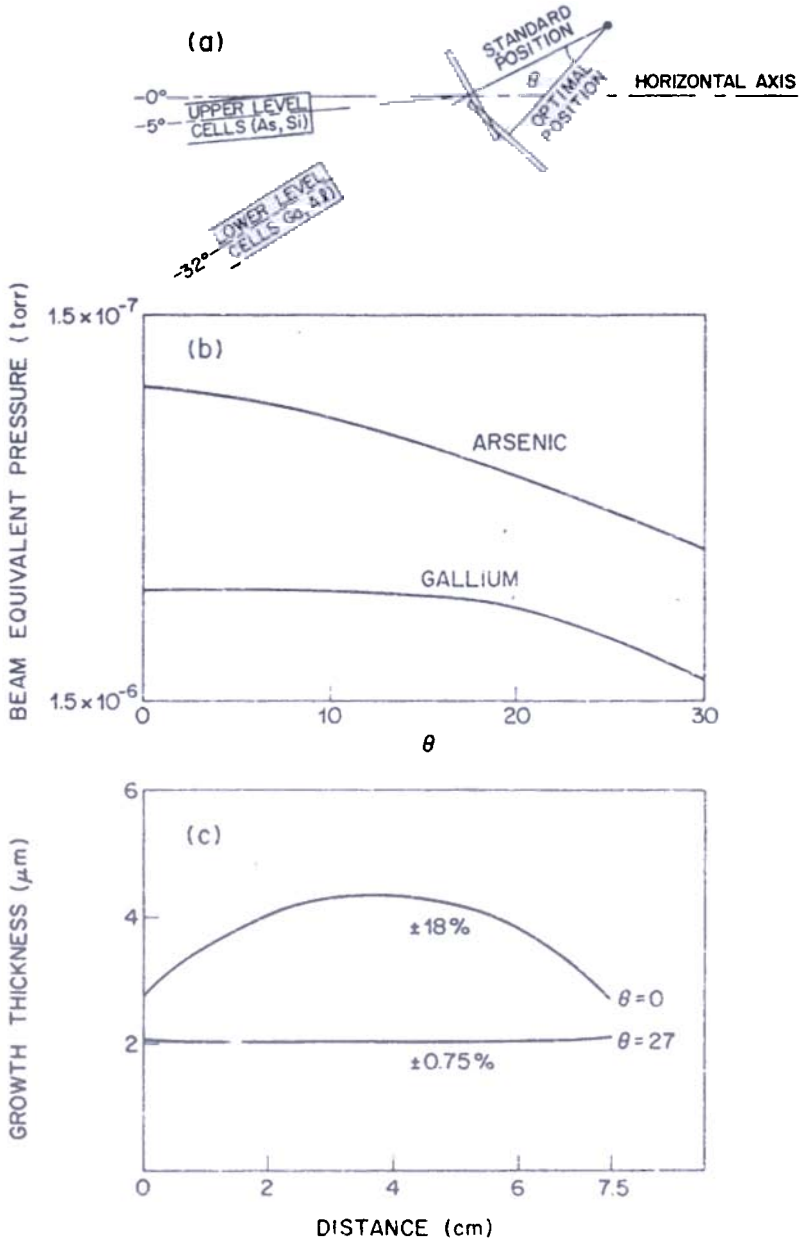


**Figure 3. (a) Vertical cross-sectional view of the growth chamber normal to the substrate illustrating the cells positions, and standard and optimum growth positions of the substrate in a Riber MBE system. (b) Variation of the BEP of *Ga* and *As* fluxes with respect to the position of the subtrate from the standard position. (c) Measured thicknesses of grown *GaAs* on 7.5 cm dia *Si* substrate at standard and optimum positions.**

has two rows of cells. The position where the axes of all the cells intersect at the center of the substrate is called the standard position. The measured angular variation of BEP of *Ga* and *As* fluxes below the standard position ($\theta = 0$) is shown in Fig. 3(b). The measured growth rate at the standard position is highly nonuniform, $\pm$ 18 per cent on a 7.5 cm dia substrate. This is shown in Fig. 3(c). Rotation of the substrate does not help at this position as the molecular beams flux remain focussed in the centre. However, when the substrate is lowered 27 degree from the standard position, the lateral growth rate uniformity is $\pm$ 0.75 per cent on the same size substrate and this uniformity can be improved by further adjustment in the position of the substrate. The uniformity obtained is, however, considered excellent and is the best ever reported. This position is called the optimum position.

As shown in Fig. 3(a), at the optimum substrate position the growth rate is about half of the maximum growth rate at the standard position. This is the result of angular variations of the fluxes shown schematically in Fig. 3(b). Notice that the *As* flux reduces at a faster rate than the *Ga* flux with increasing $\theta$. This is due to the fact that *As* is loaded in the upper level cells and *Ga* in the lower level cells. Thus, with increasing $\theta$, for given cell temperatures, *As/Ga* flux ratio decreases. For a given growth rate, the cell temperatures have to be higher for the optimum growth position, than those when the growth is at the standard position. The temperature of the *As* cell with have to be even higher. This is the price one pays for obtaining better lateral growth uniformity.

With excellent lateral uniformity and calibration of the growth rate at the optimum position, it was possible to grow the high responsivity and high detectivity bound-to-external-state quantum well detector[17] with peak response just at the targetted wavelength of 10 μm at the very first try. The transmission electron microscopy (TEM) cross-section of the structure is shown in Fig. 4. The structure has 50 *GaAs* quantum wells, each 40 Å thick, bound by 300 Å thick $Al_{0.23}Ga_{0.77}As$ barrier layers. High magnification TEM cross-sections of the same structure show nonuniformity of only $\pm$ 2 per cent in the direction of growth from period to period. This nonuniformity is also due to nonsynchronisation of the substrate rotation speed with each period of the structure. The total layer thickness was, however, just right. This work demonstrates excellent uniformity and control over the MBE growth.

Although the lateral uniformity of *AlAs* content in $Al_xGa_{1-x}As$ was also very good ($\Delta x = \pm 0.002$ for $x = 0.32$) over a 7.5 cm dia wafer, substrate rotation induced periodic variations in *AlAs* content along the direction of growth were observed[18,19]. This is shown in Fig. 5 where layers of $Al_{0.3}Ga_{0.7}As$ were grown with rotation speeds of 1, 3 and 7 rpm. The *AlGaAs* layers (bright regions) are separated by *GaAs* spacer layers (dark regions). When the rotation speed was increased to 16 rpm (not shown in Fig. 5), no such composition modulation was observed[18]. It was interesting to note that the Hall measurements and high resolution x-ray diffractometry did not show any difference in $Al_xGa_{1-x}As$ layers grown with and without substrate rotation induced composition modulation.

Within the measurement errors of $\pm$ 2 per cent, no nonuniformity in *n*- or *p*-doping density over a 7.5 cm dia substrate was detected by us.

## 8. RESIDUAL IMPURITIES AND ELECTRON MOBILITIES

High-quality *GaAs* should have a low level of background impurities and high electron mobilities. Without the former, the latter can not be achieved. Simultaneous presence of the two is an indication of the perfection of the evaporation sources and the optimum

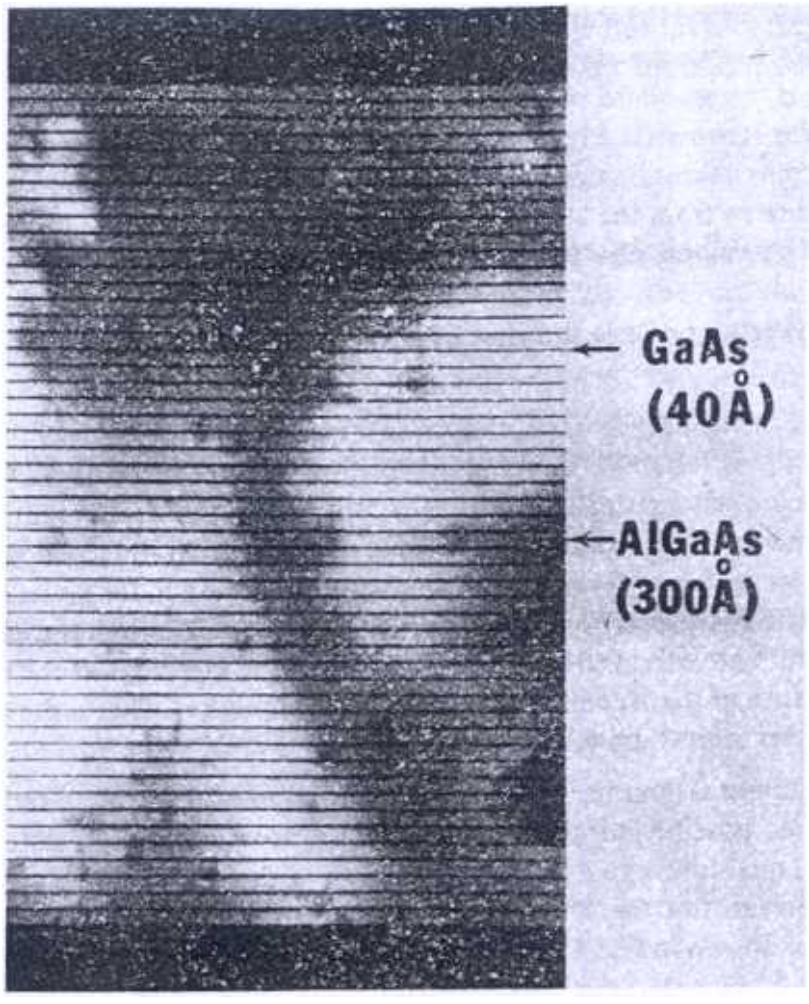


**Figure 4. TEM cross-sectional view of a 10 μm long wavelength bound-to-external-state quantum well detector. The structure comprises 50 *GaAs* quantum wells (dark lines), each 40 Å thick, bound by 300 Å thick $Al_{0.23}Ga_{0.77}As$ barrier layers (bright regions).**

growth conditions. Normally, high mobility *GaAs* layers also posses other desirable properties, such as better intrinsic luminescence characteristics and fewer defects. High electron mobilities and a low level of background impurities are important for many device applications and physical study of materials.

Unintentionally doped MBE-*GaAs* is generally *p*-type and carbon is known to be the main residual acceptor impurity. Other background acceptors are *Zn, Mn* and *Si* (on *As* site). The net background acceptor density ($N_A - N_D$) varies from system to system and, typically is low $10^{14}$ cm$^{-3}$. Larkins and coworkers[12] reduced $N_A$ to $2.4 \times 10^{13}$ cm$^{-2}$, but instead observed a residual donor concentration ($N_D$) of $1.5 \times 10^{14}$ cm$^{-3}$, apparently due to sulphur which was present in their arsenic source. When *GaAs* was grown by MBE using $AsH_3$ gas instead of solid *As*, Cunningham and coworkers[9] found their *GaAs* to be *n*-type with $N_D \sim 10^{14}$ cm$^{-3}$. Calawa *et al.*[20], who were the first to demonstrate the MBE growth of *GaAs* using $AsH_3$ gas, also found undoped *GaAs* to be *n*-type. In the present case[8], *GaAs* grown with 6N grade *As* had a very high background acceptor density which varied between $5 \times 10^{14}$ and $10^{15}$ cm$^{-3}$. Except for changing the sources, everything else which could possibly be thought of, was done to reduce $N_A - N_D$ below $10^{14}$ cm$^{-3}$ but no success was achieved. However, simply changing the *As* source to a 7N grade slug reduced $N_A - N_D$ to $10^{13}$ cm$^{-3}$. The above results therefore indicate that the *As* source is the dominant cause of

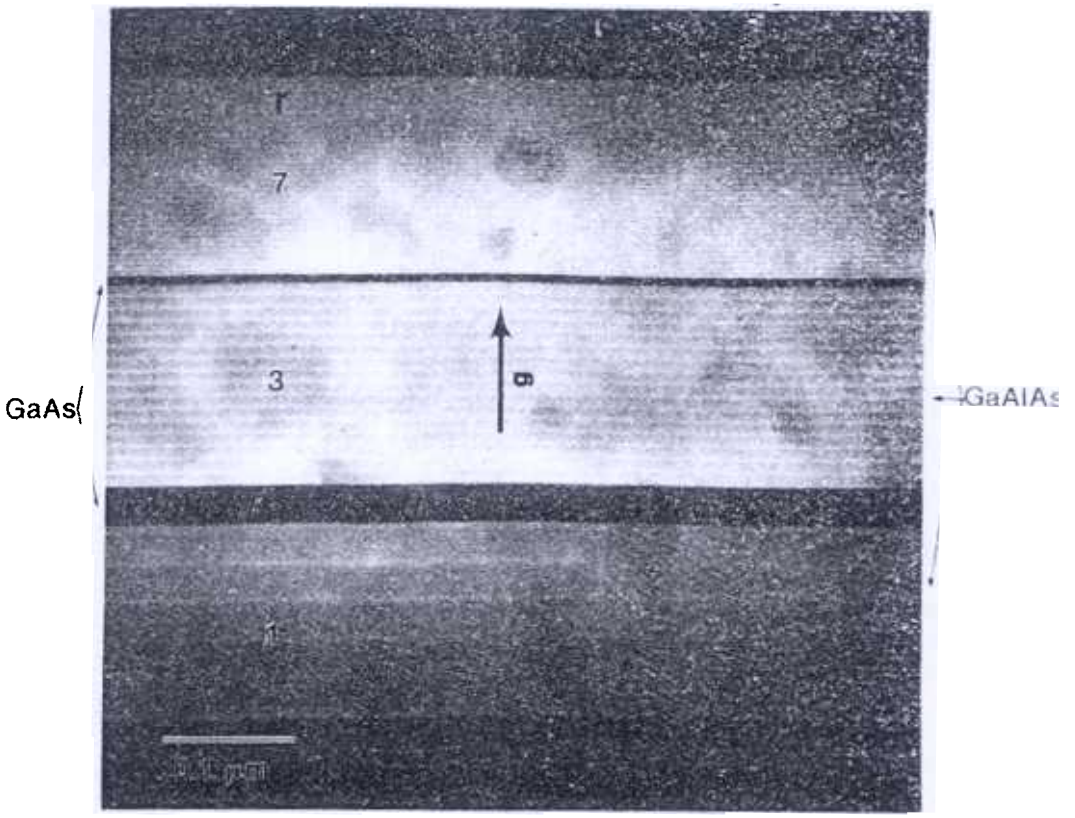


**Figure 5. A [011] XTEM micrograph of a $Al_{0.3}Ga_{0.7}As/GaAs$ multilayer structure illustrating the substrate rotation-induced fine composition modulation of *AlGaAs*.**

the residual impurities in MBE-*GaAs*, although the impurities can come from other sources also.

Figure 6(a) shows photoluminescence data at 6 K for undoped *GaAs* grown with 6N grade *As* chunks. The D°—A° peak at ~ 1.491 eV, the sharp defect-related peak near 1.506 eV and the two sharp exciton bound to donor peaks at ~ 1.514 eV all go nearly to zereo, as expected, when the temperature is increased to 29 K. In contrast, the photoluminescence in Fig. 6(b) from undoped *GaAs* grown with the *As* slug exhibits very little A°-related emission and just a hint of excitons bound to impurities near the free-exciton emission at 1.5151 eV. The ratio of exciton edge emission to the A°-related emission near 1.49 eV is more than an order of magnitude larger with the *As* slug. The excitation intensity ($I$) for Fig. 6(a) is 14 times that for Fig. 6(b), and hence there could also be some saturation of the impurity-related emission in Fig. 6(a). Two-hole transitions observed via resonant excitation with a tunable dye laser in the region of A°-$X$ at 1.5127 eV indicate in both cases that $C$ and $Zn$ are indeed the major acceptor impurities in *GaAs*.

When the background impurities are reduced, electron mobilities in lightly $n$-doped *GaAs* automatically increase. When the residual net acceptor density was $5 - 10 \times 10^{14}$ $cm^{-3}$, we could never dope *GaAs* below $10^{15}$ $cm^{-3}$ with *Si* donors, and the measured electron mobilities at 77 K ($\mu_{77K}$) were below 25,000 $cm^2V^{-1}s^{-1}$. When the background acceptor density reduced to a low $10^{13}$ $cm^{-3}$, our $\mu_{77K}$ was greater than $2 \times 10^5$ $cm^2V^{-1}s^{-1}$ and the peak mobility at 42 K was $\sim 3 \times 10^5$ $cm^2V^{-1}s^{-1}$. The corresponding electron density ($N_D - N_A$) was

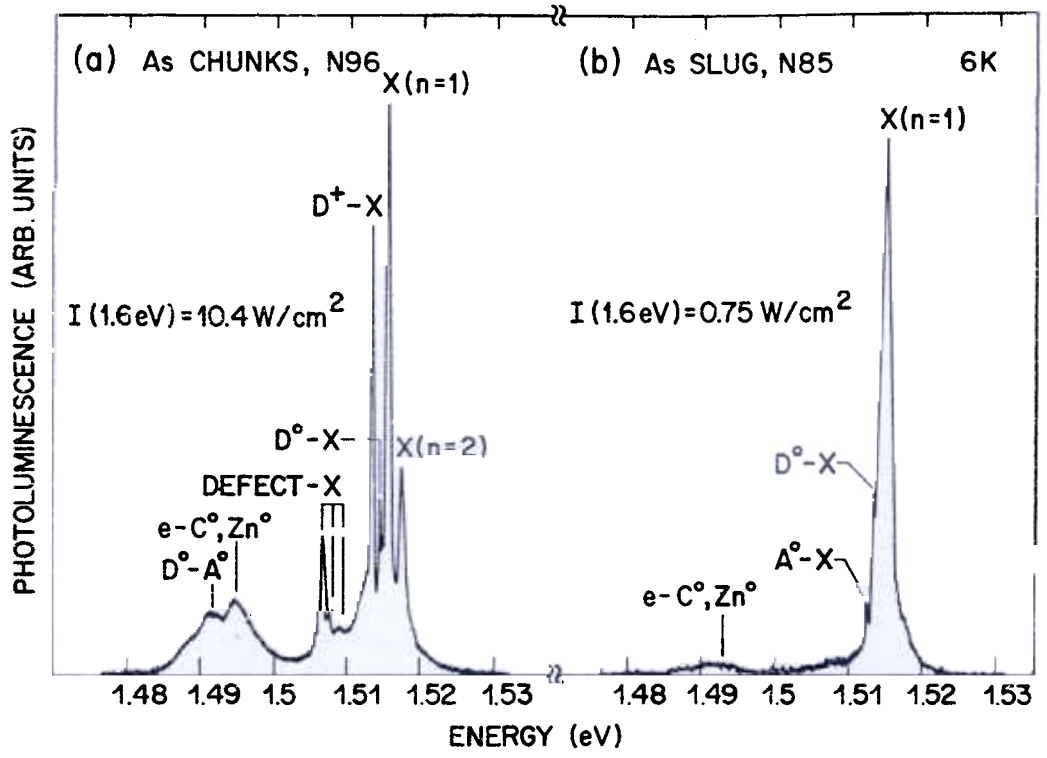


**Figure 6. Photoluminescence at 6 K for undoped *GaAs* grown using (a) 6N grade *As* chunks and (b) 7N grade *As* slug. *I* is the excitation intensity.**

$3 \times 10^{13}$ cm$^{-3}$. These mobilities are the highest ever measured in MBE-*GaAs* and are significantly larger than the previously obtained highest values, as shown in Fig. 7. The best results of vapour phase epitaxy-gallium arsenide (VPE-*GaAs*) obtained by Stillman and Wolf[21] are also shown for comparison in Fig. 7. It should be noted that because of surface and interface depletion effects[22,23], the high mobility samples are grown relatively thick, and for the same reasons there could be some errors in the doping densities shown. We, however, confirmed our doping densities by capacitance-voltage doping profiles. Also, the peak mobility in *GaAs* is normally obtained at ~ 40 K and not at 77 K, so both the 77 K and the peak mobilities (where available) are plotted in Fig. 7. Furthermore, the samples of Chand *et al.*,[8] Heiblum *et al.*,[13] and Morkoc & Cho[22] are intentionally doped with *Si*, whereas the samples of Stillman *et al.*,[21] and Larkins *et al.*,[12] are unintentionally *n*-doped. Although similar high peak electron mobility (~ $3 \times 10^5$ cm$^2$V$^{-1}$s$^{-1}$) has also been demonstrated in unintentionally *n*-doped *GaAs* grown by gas-source MBE[9] and metal organic chemical vapour deposition (MOCVD)[24], MBE-*GaAs* appears to be intrinsically purer because it has a lower level of residual impurities.

## 9. ELECTRON AND HOLE TRAPS

Some chemical impurities and crystal defects give rise to energy levels deep in the bandgap which act as traps for electrons or holes. Performance of both majority and minority carrier devices are affected by the presence of these traps. The types of traps in *GaAs* have been found to depend on the crystal growth technique used. In MBE-*GaAs*, a family of electron traps arbitrarily numbered from *M*0, *M*1, ... *M*8 has been observed[25-28] without any consensus as to their origin. Of these MBE traps, *M*1, *M*2, *M*3 and *M*4 are much more common. Although the density of these traps is relatively small ($10^{12} - 10^{14}$ cm$^{-3}$) compared to the doping densities typically used (~ $10^{17}$ cm$^{-3}$) in many devices, their presence is the symptom of defect-impurity structure in the material. In novel device

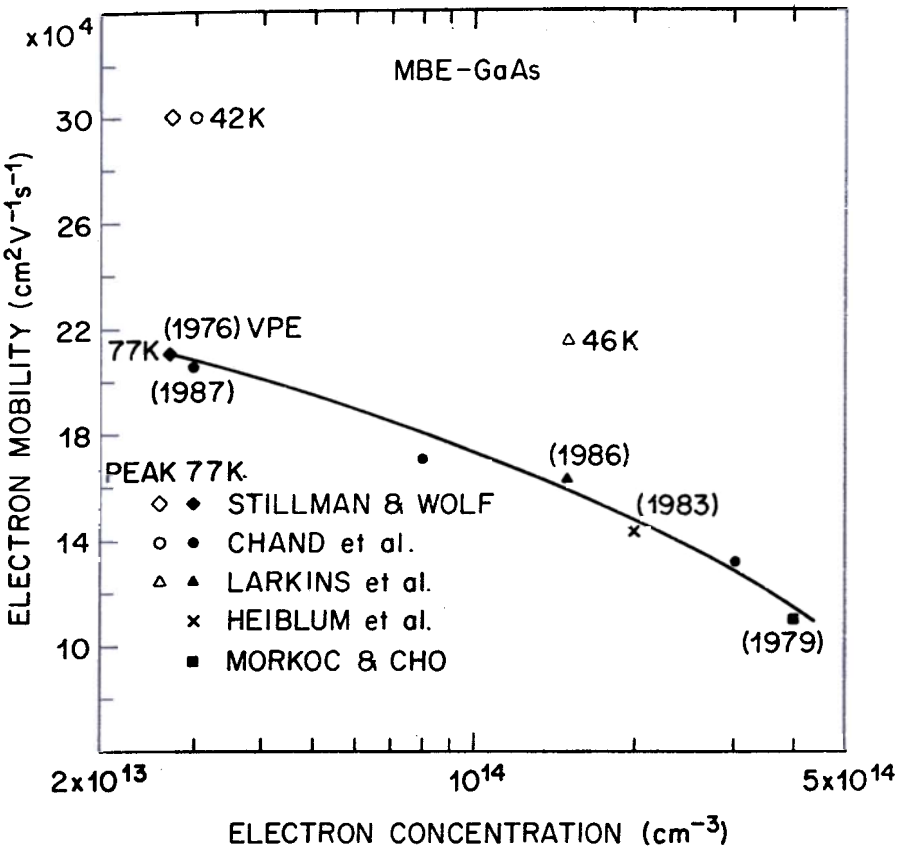


**Figure 7. Landmarks of the Hall electron mobilities in *n-GaAs* grown by MBE using solid arsenic source. The data shows continuous improvement in electron mobilities year after year.**

applications where the active region is intentionally undoped, such as in selectively-doped heterostructure transistors (SDHTs—also called MODFETs or high electron mobility transistors—HEMTs) or in devices employing thin superlattice structures, even a low trap density can have very deleterious effects. The performance of devices using material free from residual impurities and defects can be significantly better.

Techniques such as: (a) growth of *GaAs* in *Ga*-stable conditions (higher growth temperature and/or smaller $As_4/Ga$ ratio)[25-27]; (b) use of $As_2$ or $AsH_3$ in place of $As_4$ as the source of arsenic[20]; (c) adding a small amount of an isoelectronic impurity (indium) during growth[29]; (d) introduction of a small partial pressure of molecular $H_2$ ($1.2 \times 10^{-6}$ torr) during growth[30] and (e) post-growth hydrogenation treatment[31] have been used with limited success to improve the purity and to reduce or passivate the traps concentration in MBE-*GaAs*. A detailed study[32] of electron and hole traps indicates that *GaAs* grown by MBE under ideal conditions, is essentially free from electron and hole traps, and all the above techniques are unnecessary. The presence of traps as detected by deep level transient spectroscopy (DLTS) is an indication of some contamination introduced by impurities in the evaporation sources, or resulting from substandard growth conditions. In fact, any abnormality in the growth process was found to be reflected by the presence of traps. Samples which had electron traps, also had lower electron mobilities, or vice versa. DLTS can, therefore, be used as a simple and powerful diagnostic tool for monitoring the cleanliness of an MBE system and for determining optimum growth conditions.

Consistent with the mobility data discussed in the preceeding sections, as shown in Figs. 8 and 9, *GaAs* grown with 6N grade *As* has electron traps in *n-GaAs* and hole traps in *p-GaAs*. In contrast, in *GaAs* grown with a 7N grade *As* slug, none of the electron or hole traps are clearly discernable. From this and our other work[32], we find that the origin of

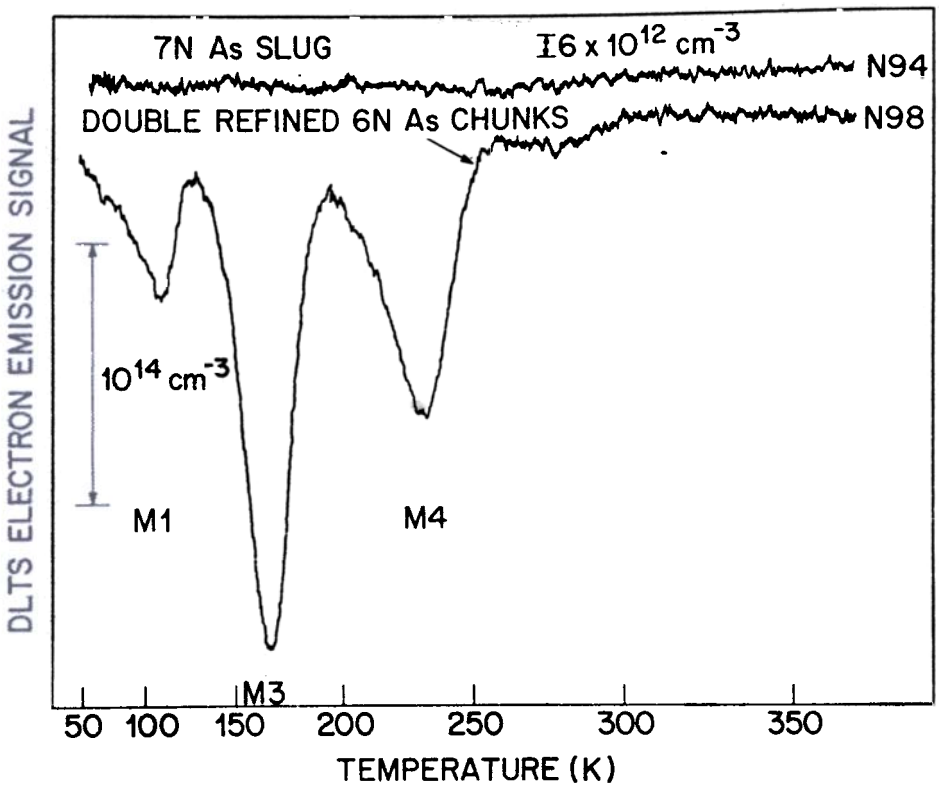


**Figure 8. DLTS spectra of electron traps in *Si*-doped *GaAs* grown by MBE using two different arsenic sources. The rate window is 50 $s^{-1}$.**

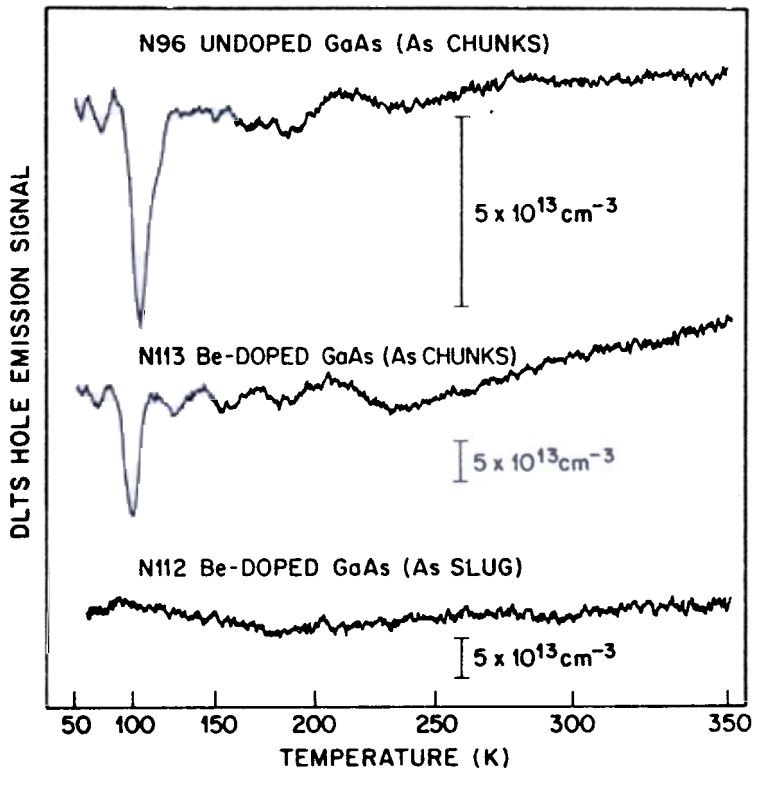


**Figure 9. DLTS spectra of hole traps is undoped and *Be*-doped *GaAs* grown by MBE using two different arsenic sources. The rate window is 50 $s^{-1}$.**

dominant MBE-*GaAs* hole traps and electron traps $M1$, $M3$ and $M4$ is the complexing of unknown chemical impurities and defects in the crystal. Impure arsenic is the major source of such chemical impurities, although these impurities can originate from other sources as well, such as improperly outgassed substrate holding *Mo* blocks. These trap-related chemical impurities do not appear to be the shallow donors or acceptors. Electron traps $M5$-$M8$ are due to crystal defects[32].

## 10. OVAL DEFECTS

The most common morphological defects, and the only remaining problem associated with MBE-grown *GaAs* films, are the so-called oval defects (after their oval shape), which are hillocks or faceted growth around nucleation centres. One such oval defect is shown in Fig. 10. The major axis of these defects is always oriented along <011>, and its size ranges

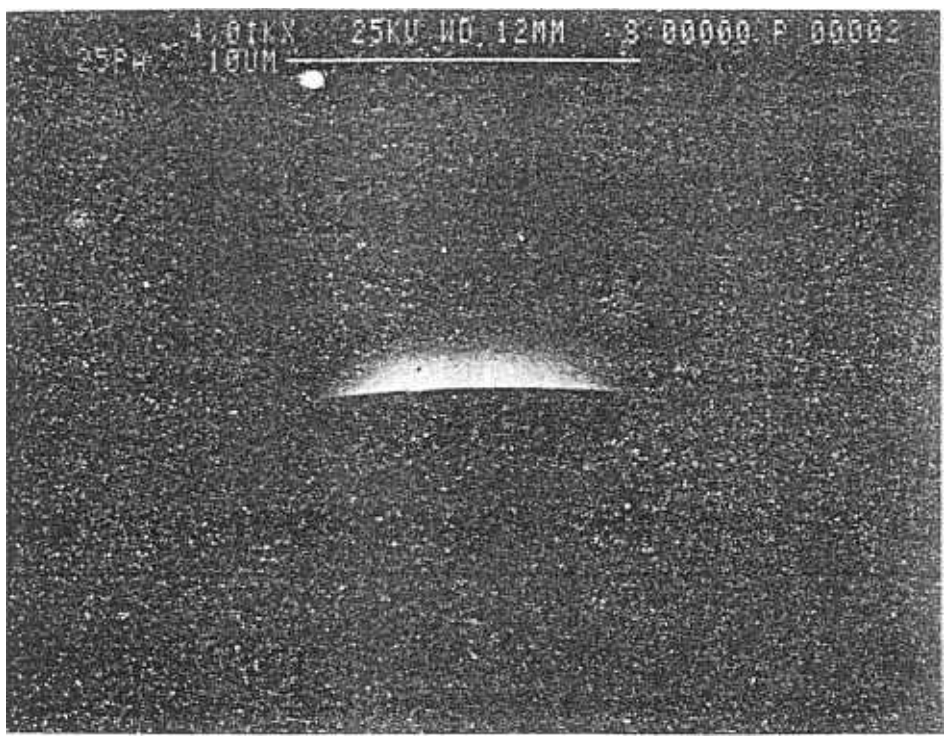


**Figure 10. A typical oval defect related to the *Ga* cell in MBE-*GaAs*.**

from 1 to 20 μm. Their density varies from $10^2$ to $10^4$ cm$^{-2}$ for films of thicknesses of 1–2 μm. Shinohara *et al.*[33] found that the breakdown voltage of a *GaAs* MESFET was degraded by the oval defect, but only when the core of the oval defect was located at the gate edge. The presence of oval defects can cause significant problems, in fabrication and reliability of large scale integrated circuits (LSIs). At this time, however, the yield of LSIs is limited by factors other than the oval defects. Our 10–15 μm thick high purity *GaAs* layers[8] had a lot of oval defects which neither affected the transport properties nor showed any trap in the DLTS study. The Schottky diodes for DLTS study had very small leakage current and high breakdown voltage and thus the exact role of oval defects in the performance of devices is still uncertain. Nevertheless, the oval defect levels must be drastically reduceed or completely elminated.

There are many possible origins for the oval defects. They can be related to substrate, particulates and the gallium source. Each category contains oval defects with a distinctive morphology. A detailed description of the oval defects and possible ways to minimise their level can be found in a number of excellent articles[34-41]. In fact, the presence of oval defects emphasizes the importance of careful preparation of the substrate, the outgassing and cleaning of the source materials, and choosing the right growth conditions.

## 11. SUMMARY

The MBE growth process and various considerations necessary in the growth of high-quality *GaAs* have been briefly discussed. It has been shown that state-of-the-art of *GaAs* can be grown by MBE. Although the progress in MBE has made it a simple crystal growth technique, there is no room for error, without cost, at any stage. Great meticulousness is essential at every stage of the MBE growth.

## ACKNOWLEDGEMENTS

It is a great pleasure to acknowledge A.Y. Cho, who taught me MBE, and my many colleagues at AT&T Bell Laboratories who have taken most of the data on MBE-*GaAs* represented in this review article. In particular, I would like to thank S.N.G. Chu for TEM cross-sections; D.V. Lang and A.M. Sergent for DLTS study; J.P. van der Ziel, R.C. Miller and S.K. Sputz-Alexander for PL study; B.F. Levine, C.G. Bethea and G. Hasnain for long-wavelength detectors; R. Fischer, D.L. Sivco, J. Walker, R.J. Malik, R.F. Kopf, and C.W. Tu for many useful discussions concerning MBE; and R.D. Yadvish and A. Savage for technical assistance. I am also grateful to my department head J.M. Gibson for encouragement and support in this work.

## REFERENCES

1. Parker, E.H.C. (Ed.), The Technology and Physics of Molecular Beam Epitaxy, (Plenum Press, New York), 1985.
2. Cho, A.Y. & Arthur, J.R., Progress in Solid State Chemistry, G. Somorjai, and J. McCaldin, (Eds.), Vol. 10, (Pergammon, New York), 1975, pp. 157-191.
3. Cho, A.Y., *J. Vac. Sci. Technol.*, **16** (1979), 275-284.
4. Ploog, K., Crystals, Growth, Properties, and Applications, H.C. Freyhardt, (Ed.), Vol. 3, (Springer-Verlag, Berlin), 1980, pp. 73-162.
5. Madhukar, A. & Ghaisas, S.V., *CRC Critical Reviews in Solid State and Material Sciences,* **14** (1988), 1-30.
6. Wood, C.E.C., *Physics of Thin Films,* **11** (1979), 35-103.
7. Proceedings of the Annual US MBE Workshops published in *J. Vac. Sci. Technol.* **B**, as well as Proceedings of the last five MBE International Conferences.
8. Chand, N., Miller, R.C., Sergent, A.M., Sputz, S.K. & Lang, D.V., *Appl. Phys. Lett.*, **52** (1988), 1721-1723.
9. Cunningham, J.E., Chiu, T.H., Timp, G.L., Agyekum, E. & Wsang, W.T., *Appl. Phys. Lett.*, **53** (1988), 1285-1287.
10. Pfeiffer, L., West, K. W., A.C., Störmer, H.L. & Baldwin, K.W., unpublished.

11. Moustakas, T.D. & Friedman, R.A., Proc. of Conf. Semiconductor-Based Heterostructure: Interfacial Structure Stability, M.L. Green, (Ed.), Metall. Soc., Warrendale, 1986, pp. 263-273.
12. Larkins, E.C., Hellman, E.S., Schlom, D.G., Harris Jr., J.S., Kim, M. H. & Stillman, G.E., *J. Cryt. Growth*, **81** (1987), 344-348, and *Appl. Phys. Lett.*, **49** (1986), 391-393.
13. Heiblum, M., Mendez, E.E. & Osterling, L., *J. Appl. Phys.*, **54** (1983), 6982-6988.
14. Foxon, C.T., Harris, J.J., Wheeler, R.G. & Lacklison, D.E., *J. Vac. Sci. Technol.*, **B4** (1986), 511-514.
15. Hwang, J.C.M, Temkin, H., Bernnan, T.M. & Frahm, R.E., *Appl. Phys. Lett.*, **42** (1983), 66-68.
16. Cho, A.Y., Private communication, and also *Thin Solid Films*, **100** (1983), 291-317.
17. Levine, B.F., Hasnain, G., Bethea, C.G. & Chand, N., To be published in *Appl. Phys. Lett.*, (1989).
18. Chu, S.N.G., Chand, N., Sivco, D.L. & Macrander, A.T., To be published *J. Appl. Phys.*, (1989).
19. Alavi, K., Petroff, P.M., Wagner, W.R. & Cho, A.Y., *J. Vac. Sci. Technol.*, **B1** (1983), 146-148.
20. Calawa, A.R., *Appl. Phys. Lett.*, **38** (1981), 701-703.
21. Stillman, G.E. & Wolfe, C.M., *Thin Solid Films*, **31** (1976), 69-88.
22. Morkoc, H. & Cho, A.Y., *J. Appl. Phys.*, **50** (1979), 8413-8416.
23. Chandra, A., Wood, C.E.C., Woodard, D.W. & Eastman, L.F., *Solid State Electron.*, **22** (1979), 645-650.
24. Shastry, S.K., Zemon, S., Kenneson, D.G. & Lambert, G., *Appl. Phys. Lett.*, **52** (1988), 150-152.
25. Lang, D.V., Cho, A.Y., Gossard, A.C., Ilegems, M. & Wiegmann, W., *J. Appl. Phys.*, **47** (1976), 2558-2564.
26. Blood, P. and Harris, J.J., *J. Appl. Phys.*, **56** (1984), 993-1007.
27. Xu, H-D., Anderson, T.G., & Westin, J.M., *J. Appl. Phys.*, **62** (1987), 2186-2187.
28. Chand, N., Fischer, R., Sergent, A.M., Lang, D.V., Pearton, S.J. & Cho, A.Y., *Appl. Phys. Lett.*, **51** (1987), 1013-1015.
29. Bhattacharya, P.D., Dhar, S., Berger, P. & Juang, F-Y., *Appl. Phys. Lett.*, **49** (1986), 470-472.
30. Pao, Y-C., Liu, D., Lee, W.S. & Harris, S.S., *Appl. Phys. Lett.*, **48** (1986), 1291-1293.
31. Dautremont-Smith, W.C., Nability, J.C., Swaminathan, V., Stavola, M., Chevallier, J., Tu, C.W. & Pearton, S.J., *Appl. Phys. Lett.*, **49** (1986), 1098-1100.
32. Chand, N., Sergent, A.M., van der Ziel, J.P. & Lang, D.V., To be published in *J. Vac. Sci. Technol.* **B**, March/April (1989).
33. Shinohara, M., Ito, T., Wada, K. & Imamura, Y., *Jpn. J. Appl. Phys.*, **23** (1984), L371-L373.
34. Wood, C.E.C., Rathbun, L., Ohno, H. & DeSimone D., *J. Crystal Growth*, **51** (1981), 299-303.

35. Akimoto, K., Dohsen, M., Arai, M. & Watanabe, N., *J. Crystal Growth,* **73** (1985), 112–117.

36. Pettit, G.D., Woodall, J.M., Wright, S.L., Kirchner, P.D. & Freeouf, J.L., *J. Vac. Sci. Technol.*, **B2** (1984), 241–242.

37. Weng, S-L., Webb, C., Chai, Y.G. & Bandy, S.G., *J. Electron. Mat.*, **15** (1986), 267–271.

38. Fukjiwara, K., Kanamoto, K., Ohta, Y.N., Tokuda, Y. & Nakayama, T., *J. Crystal Growth,* **80** (1987), 104–112.

39. Papadopoulo, A.C., Alexandre, F. & Bresse, J.F., *Appl. Phys. Lett.*, **52** (1988), 224–226.

40. Salokatve, A., Varrio, J., Lammasniemi, J., Asonen, H. & Pessa, M., *Appl. Phys. Lett.*, **51** (1987), 1340–1342.

41. Matteson, S. & Shih, H.D., *Appl. Phys. Lett.*, **48** (1986), 47–49.